Carcinogenesis, 2020, Vol. 41, No. 8, 1104–1112

doi:10.1093/carcin/bgz175
Advance Access Publication October 24, 2019
Original Article

ORIGINAL ARTICLE

Kras mutations and *PU.1* promoter methylation are new pathways in murine radiation-induced AML

Gráinne O'Brien[1], Lourdes Cruz-Garcia[1], Joanna Zyla[2,*], Natalie Brown[1], Rosemary Finnon[1], Joanna Polanska[2] and Christophe Badie[1]

[1]Public Health England, Centre for Radiation, Chemical and Environmental Hazards, Oxfordshire, UK and [2]Silesian University of Technology, Data Mining Division, Gliwice, Poland

*To whom correspondence should be addressed. Tel: +44 01235 825088; Email: Christophe.Badie@phe.gov.uk

Abstract

Therapy-related and more specifically radiotherapy-associated acute myeloid leukaemia (AML) is a well-recognized potential complication of cytotoxic therapy for the treatment of a primary cancer. The CBA mouse model is used to study radiation leukaemogenesis mechanisms with *Sfpi1/PU.1* deletion and point mutation already identified as driving events during AML development. To identify new pathways, we analysed 123 mouse radiation-induced AML (rAML) samples for the presence of mutations identified previously in human AML and found three genes to be mutated; *Sfpi1* R235 (68%), *Flt3*-ITD (4%) and *Kras* G12 (3%), of which G12R was previously unreported. Importantly, a significant decrease in *Sfpi1* gene expression is found almost exclusively in rAML samples without an *Sfpi1* R235 mutation and is specifically associated with up-regulation of *mir-1983* and *mir-582-5p*. Moreover, this down-regulation of *Sfpi1* mRNA is negatively correlated with DNA methylation levels at specific CpG sites upstream of the *Sfpi1* transcriptional start site. The down regulation of *Sfpi1/PU.1* has also been reported in human AML cases revealing one common pathway of myeloid disruption between mouse and human AML where dysregulation of *Sfpi1/PU.1* is a necessary step in AML development.

Introduction

After exposure to ionizing radiation (IR), acute myeloid leukaemia (AML) is one of the most common malignancies to occur in humans (1). AML can also be induced by therapy treatments such as radiotherapy, so-called secondary or therapy-related AML (t-AML). In comparison with *de novo* AML, t-AML is a disease with a faster onset and often resistance to chemotherapy, higher relapse rates and lower overall survival rates (2). There is a growing incidence of t-AML due to an ageing population, increased detection and treatment of cancers treated by chemotherapy and/or radiotherapy. Therefore, investigation into the development of t-AML, the genetic factors associated with risk of development of t-AML and improved treatment options are vital for the successful treatment of these patients.

Several strains of mice have been used to study rAML, such as CH3/He, RF and SJL/J, with the inbred CBA strain being the best characterized model of radiation induced AML. CBA mice have low-background rates of AML (<1 in 1000) (3), there is a consistent induction rate of 15–20% following exposure to an optimal leukaemic dose of 3 Gy whole-body exposure (4,5) and the histopathological features, such as splenomegaly, are very similar to that of human AML. In this rAML model, AML develops after irradiation mainly through the deletion of one *Sfpi1* allele. *Sfpi1* is also known as the myeloid transcription factor *PU.1* in humans. In about 90% of mice that develop rAML, a partial deletion of one copy of chromosome 2 was identified (6), always containing *Sfpi1*. This is commonly thought of as the first event in radiation leukaemogenesis. In mice carrying chromosome 2 deletions, 70–80% were found to additionally carry a point mutation at codon R235 on the remaining allele of *Sfpi1* in the DNA-binding domain of the protein (7) which is believed to be the second molecular event required for leukaemia development. This mechanism seems to be highly specific to this mouse model and one that is not commonly found in human tAML

Received: 13 June 2019; **Revised:** 17 September 2019; **Accepted:** 21 October 2019

Abbreviations

AML	acute myeloid leukaemia;
IR	ionizing radiation;
CGH	comparative genomic hybridization;
rAML	radiation-induced AML;
t-AML	therapy-related AML;
URE	upstream regulatory element

cases (8). The incidence of this mechanism in human cases of radiation induced AML, however, is not known as most tAML cases contain a mix of radiotherapy and chemotherapy.

The use of the CBA mouse has been recognized as a good model of leukaemogenesis with a recent review highlighting the important role of *PU.1* in leukaemogenesis in both human and mouse AML cases (5). Although a *PU.1* R235 mutation is a rare event in human AML, recent studies have reported a reduced expression of *PU.1* clearly evident in *de novo* AML cases (9,10). The dysregulation of *PU.1* seems to be common to both murine and human cases. Repression of *Sfpi1*, through epigenetic mechanisms, may also occur in unmutated cases in CBA mice, supporting the use of the CBA mouse as a model of leukaemogenesis.

Epigenetic genes such as *DNMT3A*, *IDH1*, *IDH2*, have recently been identified as a new category of genes mutated in AML (11) and epigenetic mutations have not yet been fully investigated in murine rAML. In this study, we screened 123 murine rAML samples to search for specific hotspot of mutations in the gene *PU.1* and also *Dnmt3a*, *Idh1*, *Idh2*, *Flt3*, *Npm1*, *Kras*, *Nras*, *C Kit* and *Cepba* which are commonly mutated in human AML cases (11) and to identify potential epigenetic changes associated with leukaemogenesis.

Materials and methods

Mouse samples

A bank of 123 rAML samples (19 DNA samples and 104 spleen samples) were held at PHE, Chilton, Oxfordshire as detailed in Supplementary Table S1, available at *Carcinogenesis* Online. The samples were a combination of 95 CBA/H mice, 30 exposed to 3 Gy X-rays, 3 exposed to 4.5 Gy X-rays and 62 exposed to neutrons and 28 F1 CBA/H × C57BL/Lia mice exposed to 3 Gy X-rays. The F1 CBA/H × C57BL Lia background mice were irradiated and characterized at NRG, Petten, Netherlands as described previously (6). The X-ray induced CBA/CaH AML mice were induced and characterized at Public Health England, Chilton, Oxfordshire as described previously (12). Mice were irradiated at MRC Harwell using a Pantak X-ray source 250 kVp, 11 mA at a dose rate of 0.887 Gy/min to give a single whole-body dose. The 62 neutron-induced AMLs were irradiated with fast fission neutrons from a 235U converter in the Low Flux Reactor at NRG, Petten, Netherlands, as described previously (13). AMLs were diagnosed using the criteria described in the Bethesda Proposals for Classification of Non-lymphoid Hematopoietic Neoplasms in Mice (14). All animals were bred and handled according to UK Home Office Animals (Scientific Procedures) Act 1986 and with guidance from the local animal welfare body. All spleen samples had been stored in RNALater (Thermo Fisher Scientific, Paisley, UK) at the time of sacrifice.

Nucleic acid extraction

RNA was extracted from spleen tissues using the miRNeasy Mini Kit (Qiagen Ltd, Crawley, UK) and DNA was extracted from spleen tissue using the DNeasy® Blood & Tissue kit (Qiagen Ltd) according to manufacturer's guidelines. RNA and DNA quantity were measured using the NanoDrop 2000 spectrophotometer (Thermo Fisher Scientific) and quality assessed using the 2200 TapeStation (Agilent Technologies Ltd, Wokingham, UK) according to manufacturer's protocol.

Array comparative genomic hybridization

Comparative genomic hybridization (CGH) analysis was performed on 116 samples as described previously (13).

Mutation detection—sanger sequencing

Primers were designed to amplify the area of interest using IDT software Primer Quest and validated by SYBRGreen analysis (Supplementary Table S2 is available at *Carcinogenesis* Online). For the PCR reaction, 1 µl of extracted DNA (25 ng DNA/µl) was placed in 9 µl PCR master mix [1 µl ×10 PCR buffer, 2 µl ×5 Q-solution, 1.6 µl 1.25 mM dNTP, 3.15 µl dH_2O, 0.5 µl 10 µM primer 'Forward', 0.5 µl 10 µM primer 'Reverse', 0.25 µl *Taq* DNA Polymerase (Qiagen, Manchester, UK). Cycling conditions were as follows: 4 min at 95°C, 35 cycles of 30 s at 95°C, 30 s at 57°C and 30 s at 72°C, followed by 10 min at 72°C. PCR products were sent for sequencing to Source BioScience (University of Oxford, UK). Sequencing files were analysed using Chromas 2.6 software (Technelysium Pty Ltd, Brisbane, Australia). PCR products were run on 2% agarose gels to allow for the detection of insertions by an increase in amplicon size.

Reverse transcription

mRNA

Reverse transcription reactions were performed using a High-Capacity cDNA Reverse Transcription Kit (Applied Biosystems, Foster City) according to the manufacturer's protocol. Cycling conditions were as follows: 25°C for 10 min, 37°C for 120 min and 85°C for 5 min.

miRNA

To prepare miRNA samples for first strand cDNA synthesis, samples were first polyadenylated using the qScript™ microRNA cDNA Synthesis Kit (Quanta BioSciences, Gaithersburg). A mixture of 100 ng RNA in 7 µl RNase-free water, 2 µl Poly(A) Tailing buffer and 1 µl Poly(A) polymerase was placed in a thermocycler at 37°C for 20 min and 70°C for 5 min. A 10 µl cDNA synthesis master mix consisting of 9 µl cDNA buffer and 1 µl reverse transcriptase was added to each sample. Cycling conditions were as follows: 42°C for 20 min and 85°C for 5 min. Samples were then diluted 50 times before QPCR analysis.

Quantitative real time-PCR

TaqMan multiplex QPCR

Real-time PCR was performed using a Rotor-Gene Q (Qiagen). Reactions were run in triplicate with primer and probe sets (Supplementary Table S2 is available at *Carcinogenesis* Online) for target genes at 300 nM each and 2.5 µl cDNA in 30 µl reaction volume (PerfeCTa® MultiPlex qPCR SuperMix; Quanta BioSciences). 3′,6-Carboxyfluorescein (FAM)/Black Hole Quencher 1 (BHQ1), 6-hexachlorofluorescein (HEX)/BHQ1, Texas Red (TEX)/BHQ2, CY5/BHQ3, Atto 680/BHQ3 and Atto 390/Deep Dark Quencher 1 (DDQ1) (Eurogentec Ltd, Fawley, UK) were used as fluorochrome reporters for the hydrolysis probes analysed in multiplexed reactions. Cycling parameters were as follows: 2 min at 95°C and 45 cycles of (10 s at 95°C and 60 s at 60°C). Data were collected and analysed using Rotor-Gene Q Series software. Gene target cycle threshold (C_t) values were normalized to an internal control (*Hypoxanthine-Guanine phosphoribosyltransferase 1; Hprt*). C_t values were converted to transcript quantity using standard curves obtained by serial dilution of PCR-amplified DNA fragments of each gene and run in each reaction. The linear dynamic range of the standard curves covering six orders of magnitude (serial dilution from 3.2×10^{-4} to 8.2×10^{-10}) gave PCR efficiencies between 93% and 103% for each gene with $R^2 > 0.998$.

miRNA QPCR

miRNA QPCR was performed using a Rotor-Gene Q (Qiagen). miScript Primer Assays were used for each miRNA of interest (Qiagen). Assay reactions of 10 µl contained 5 µl PerfeCTa SYBR® Green SuperMix (Quanta BioSciences), 0.3 µl Universal primer (Quanta BioSciences), 0.3 µl Assay primer, 3.4 µl RNase-free water and 1 µl cDNA. Cycling conditions were as follows: 95°C for 2 min, 45 cycles of 95°C for 10 s and 60°C for 30 s followed by a melt curve. Data were analysed using Rotor-Gene Q Series software.

nCounter miRNA analysis

Bioanalyser miRNA measurement

The miRNA quantity was measured using the Small RNA Analysis Kit (Agilent Technologies Ltd) according to manufacturer's instructions. The chip was run on the Agilent 2100 Bioanalyzer instrument (Agilent Technologies Ltd).

nCounter miRNA assay

Mouse spleen RNA was screened for the expression of 611 miRNA using the nCounter Mouse v1.5 miRNA Expression Assay Kit (NanoString Technologies®, Seattle, WA) on the nCounter Analysis System (NanoString Technologies®) according to the manufacturer's guidelines. Data were analysed using the nSolver software and BRB-ArrayTools. BRB-ArrayTools was developed by Dr Richard Simon and the BRB-ArrayTools Development Team.

Pyrosequencing

Mutational analysis

Novel mutations were confirmed by pyrosequencing using the Pyromark Q48 according to manufacturer's guidelines. Briefly, primers for mutational analysis were designed by the Pyromark Q48 Advanced Software (Supplementary Table S2 is available at *Carcinogenesis* Online) and amplified by PCR using Pyromark Q48 Advanced Reagents and Magnetic Beads (Qiagen).

DNA methylation analysis

DNA methylation was analysed by pyrosequencing using the Pyromark Q48 (Qiagen) according to manufacturer's guidelines. Briefly, bisulfite conversion was performed on 1 µg DNA using the EpiTect Fast Bisulfite Conversion Kit (Qiagen). Briefly, 140 µl bisulfite reactions were prepared with 20 µl DNA, 85 µl bisulfite solution and 35 µl DNA protect buffer (Thermo Fisher Scientific). Cycling conditions were as follows: 95°C for 5 min, 60°C for 20 min, 95°C for 5 min and 60°C for 20 min. Primers for methylation analysis were designed by the Pyromark Q48 Advanced Software (Supplementary Table S2 is available at *Carcinogenesis* Online) and DNA methylation analysis was then performed on the PyroMark after PCR amplification.

Statistical analysis

The deleterious impact of observed mutations to encoded amino acid in *Kras* protein was checked using PredictSNP (15) and PolyPhen-2 (16) algorithms. The reference *Kras* FASTA sequence was NP_067259.4. Gene expression and DNA methylation data were analysed using the statistical method Mann–Whitney using Minitab18. Fishers exact test for proportions was used to calculate significance for gender differences using Minitab18. The calculation for the presence of an *Flt3*-ITD includes the four females mice with an *Flt3*-ITD in this study and a fifth female mouse with an *Flt3*-ITD from Finnon et al. (17).

Results

Identification of commonly mutated human AML genes in murine rAML

Mutated cases were found for three genes in the panel of mouse samples screened; mutations at codon R235 in *Sfpi1/PU.1*, insertions at exon 14 in *Flt3* and mutations at codon G12 in *Kras* as detailed in Table 1, available at *Carcinogenesis* Online, with accompanying CGH data. No mutations were found in the remaining locations sequenced.

Sfpi1 mutations of the codon R235 were found to be the most commonly mutated gene with a total of four different types of missense mutations affecting codon R235 and one silent mutation affecting codon L234, in total affecting 68% of all cases. *Flt3* was the next most commonly mutated gene with four different insertions in four CBA mice in total (Figure 1). Two of these *Flt3*-ITDs have been previously reported by our group in

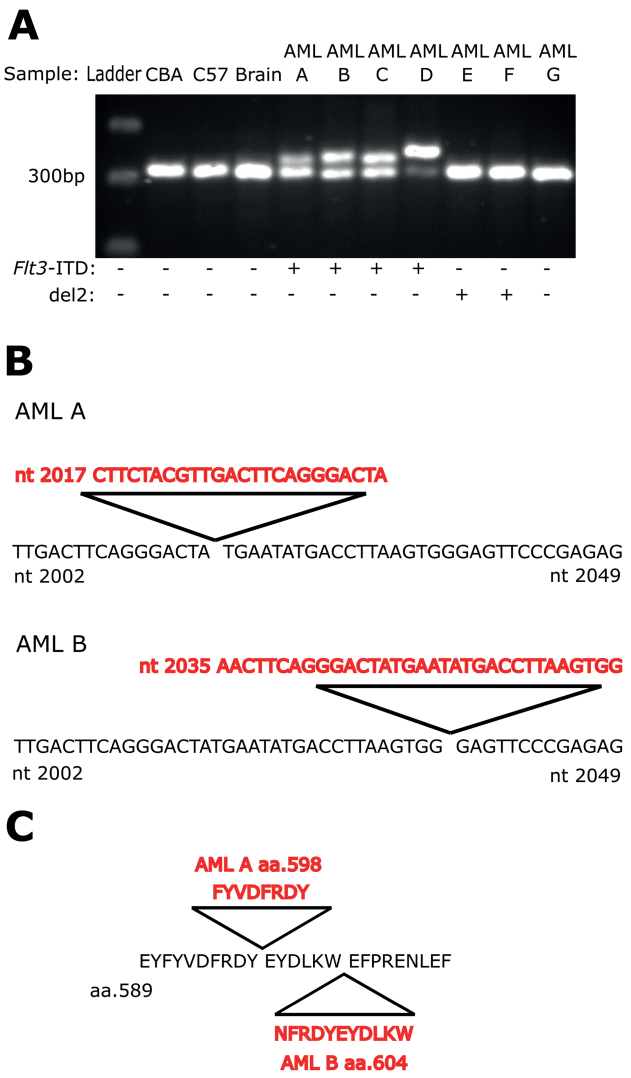

Figure 1. Analysis of *Flt3*-ITD in murine rAMLs. (**A**) Agarose gel electrophoresis of *Flt3*-ITD PCR of a panel of murine rAMLs on a 2% gel. A normal amplicon is represented by a single band of 333 bp whereas *Flt3*-ITD has an additional larger band. The gel is loaded as indicated in the image. A cropped version of the gel is displayed. `CBA' and `C57' refer to normal spleen DNA from CBA/H and C57BL6, respectively; `Brain' refers to brain tissue from the animal in which AML A developed and represents a normal tissue control; and AMLs E–G refer to independent AML samples. *Flt3*-ITDS in AMLs C and D have been previously analysed in Finnon et al. (17). The presence or absence of an *Flt3*-ITD and chromosome 2 deletion are stated below the gel for each sample (*Flt3*-ITD: + presence and – absence; del2: + presence and – absence. (**B**) CBA sequence of exon 14 on chromosome 5 showing *Flt3*-ITDs in AML A at nucleotide 2017 (24 bp) and in AML B at nucleotide 2035 (33 bp). (**C**) Predicted CBA *Flt3* protein sequence with ITDs of AML A (aa.598) and AML B (aa.604).

Finnon et al. (17). This previous study also included a fifth *Flt3*-ITD case, which we could not use for further study in this work due to a lack of DNA availability. Importantly, this mutation appears in a significantly female pathway, occurring in five female mice in total when combining the two studies, with no male case found ($P = 0.0045$). It is still significant when considering this study alone ($P = 0.013$). Mutations in the gene *Kras* were also found in three mice, two had *Kras* G12D mutations alongside *Sfpi1* R235C mutations and one had a G12R mutation, previously unreported in the CBA mouse, with no *Sfpi1* mutation. Data mining assessment of *Kras* G12D and G12R mutations reported

a predicted deleterious impact for protein function using both PolyPhen2 (possibly damaging/Sens = 0.75/Spec = 0.87) and PredictSNP (deleterious: 87%) algorithms. PolyPhen-2 calculated 75% sensitivity and 87% specificity in the prediction of the deleterious effect for both amino acid changes. Although PolyPhen-2 tested the amino acid conservation in the human organism, PredictSNP was run to verify these findings for the mouse model. The PredictSNP algorithm confirmed PolyPhen-2 predictions with 87% confidence. Thus, using two independent bioinformatic methods, we expect a strongly deleterious impact on protein function from the observed mutations.

The three mouse samples with *Kras* mutations were confirmed by pyrosequencing (Figure 2). The frequencies of the *Sfpi1* mutations were 70% with the frequency of the *Kras* mutations being lower at 30–46%.

Significant reduction of *Sfpi1* expression evident in wild-type *Sfpi1* R235 AML

Wild-type *Sfpi1* R235 samples had, on average, a clearly significantly lower transcriptional expression level of *Sfpi1* when compared with samples with a R235 mutation (Figure 3A). Among the 3 *Kras* mutation cases, the two which had an *Sfpi1* R235 mutation (case 1 and case 2) had a level of *Sfpi1* expression similar to control levels, whereas the wild-type *Sfpi1* R235 (case 3) had a very low level of *Sfpi1* expression.

Identification of novel microRNA upregulated in *Sfpi1* R235 mutated AML

nCounter screening of miRNA identified 2 miRNA differentially expressed in samples with or without *Sfpi1* mutations, *miR-582-5p* and *miR-1983*, where $P \leq 0.05$. These were confirmed by QRT-PCR with an up-regulation of *miR-582-5p* (2-fold) and *miR-1983* (4-fold) in *Sfpi1* R235 mutated cases (Figure 3B and C). *miR-155*, a known *Sfpi1* negative regulator, is significantly up-regulated in both *Sfpi1* mutated and unmutated cases in comparison with the controls. QRT-PCR analysis shows a slight up-regulation of *miR-155* in wild-type *Sfpi1* R235 in comparison with mutated *Sfpi1*, although it is not significant (Figure 3D).

DNA methylation levels are higher at CpGs upstream of *Sfpi1* in wild-type R235 cases

DNA methylation was studied at specific CpG sites in the promoter and an upstream regulatory element (URE) of *Sfpi1* known to regulate its expression (18–20). Methylation levels were significantly higher at each of the five CpGs in the URE and the four CpGs in the promoter region in wild-type *Sfpi1* R235 when

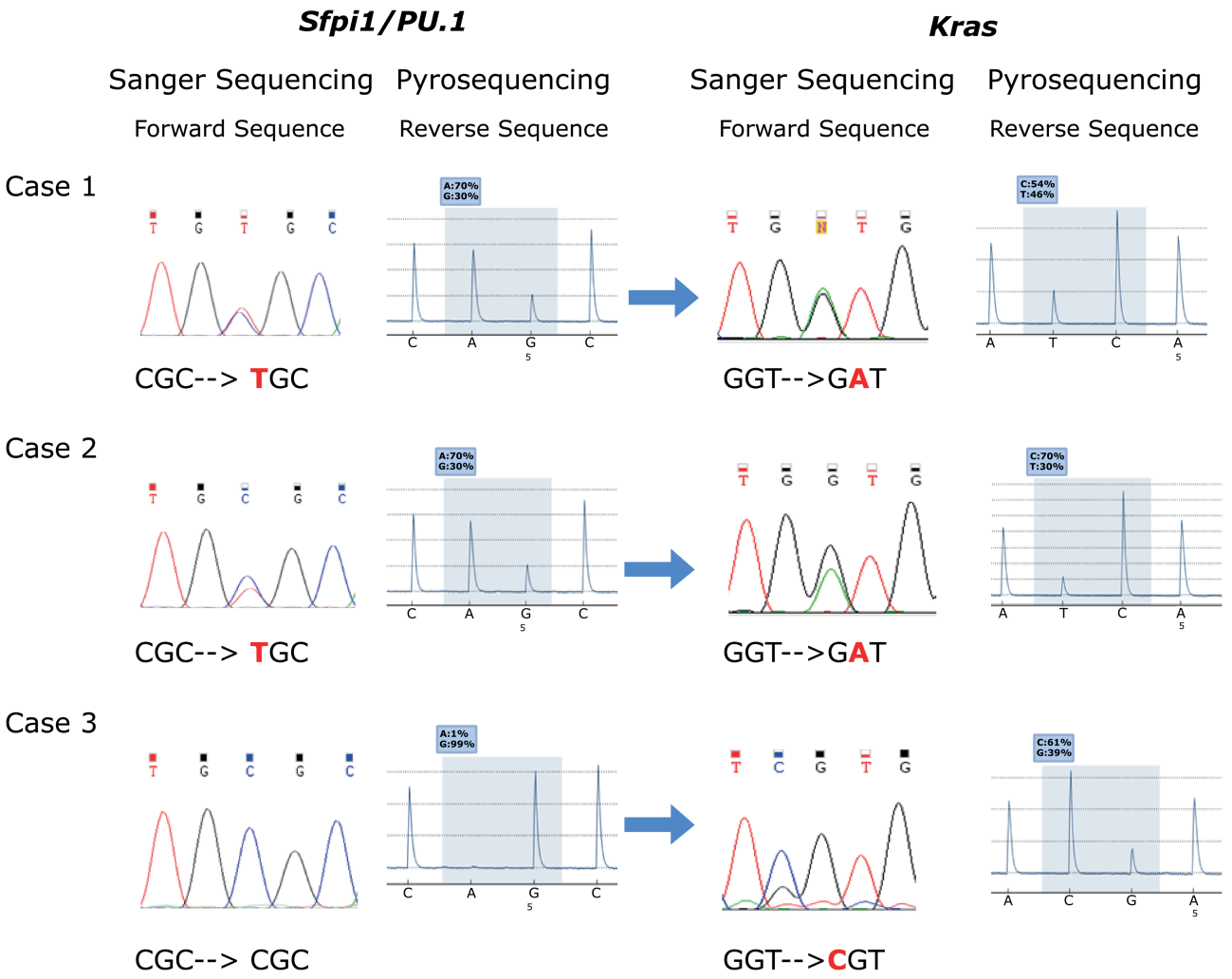

Figure 2. Analysis of *Sfpi1/PU.1* R235 and *Kras* G12 codons by sanger sequencing and pyrosequencing in three rAML mice. Case 1 and case 2 have *Sfpi1* R235C mutations of CGC→TGC and *Kras* G12D mutations of GGT→GAT, whereas case 3 was unmutated for *Sfpi1* but has a *Kras* G12R mutation of GGT→CGT.

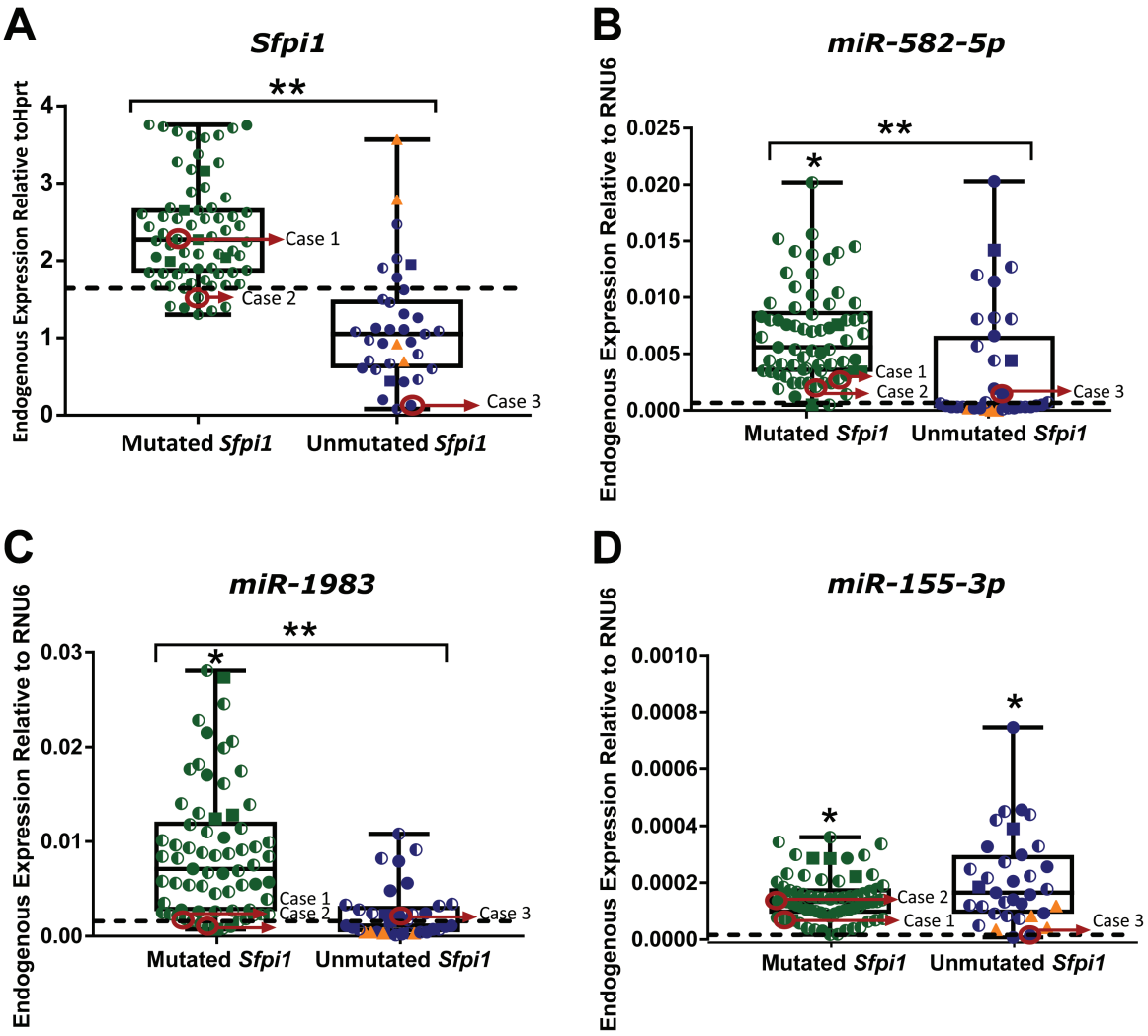

Figure 3. MQRT-PCR expression of (**A**) *Sfpi1*, (**B**) *miR-582-5p*, (**C**) *miR-1983* and (**D**) *miR-155-3p* in murine rAML samples. The box plot shows expression analysed in 3 CBA bone marrow control samples (dashed line median expression), 69 samples mutated in codon R235 (green circles) and 35 wild-type codon R235 samples (blue circles) including 4 samples with an *Flt3*-ITD (orange triangles). Chromosome 2 deletion information is also represented by a half full circle whereas samples with unknown chromosome 2 information are represented by a square box. Cases 1–3, as depicted in Figure 2, are circled in red. Expression levels were normalized to *Hprt* for mRNA and *Rnu6* for miRNA. Significance was calculated by performing a Mann–Whitney test on gene expression data and indicated with an asterisk (* $P \leq 0.05$, ** $P \leq 0.001$).

compared with samples with a R235 *Sfpi1* mutation (Figure 4). The increase in DNA methylation levels had no correlation to age at sacrifice (Supplementary Table S1 is available at *Carcinogenesis* Online). Correlation analysis showed an inverse relationship between DNA methylation level and *Sfpi1* transcriptional expression, for CpG 4 and 5 in the URE and CpG 3 in the promoter (Supplementary Figure S1 is available at *Carcinogenesis* Online).

Discussion

Identification of commonly mutated human AML genes in CBA rAML

A high frequency (90%) of *Sfpi1* chromosome 2 deletions has previously been reported to occur in rAML cases, with R235 mutations in 70% of these (6,7). Here, in the largest study to be reported so far to our knowledge, we report a lower level of chromosome 2 deletions, 81% in samples analysed by CGH, with 89% of them also containing a R235 mutation. Chromosome 2 deletions were not affected by radiation type which has also been demonstrated in a previous study (13). When comparing the presence of a chromosome 2 deletion relative to gender, deletions were identified in 61 out of 65 male mice and in 27 out of 37 female mice. A two-sample *t*-test between proportions showed a significant difference in the presence of chromosome 2 deletions between gender ($P = 0.006$). However, it is worth considering that this significance may be influenced by the four female mice with *Flt3*-ITDs, all of which have no chromosome 2 deletions and when removed from the study, result in no significant difference in chromosome 2 deletions between gender. *Flt3*-ITD mutations are rare, occurring in 4% of cases; and it is a significantly female specific pathway which occurs mutually exclusively to *Sfpi1* deletion and mutation. In human AML cases, however, *FLT3*-ITDs occur at a similar rate in female and male cases (21,22). *Kras* G12 mutations were also a rare mutational pathway occurring in 2% of all samples which is within range of the rates in human AML of 1.5% (23), 5%, 7% (24,25) and 9% (26). Two cases had a *Kras* G12D mutation which has been previously reported in mouse lymphomas (27) and $Kras^{G12D}$ mice have been shown to develop a lethal haematopoietic disease characterized

Table 1. List of the mutations and associated protein change found by Sanger sequencing in the DNA of 123 mice diagnosed with rAML, the number of mice the mutations were found to be present in and chromosome 2 deletion information obtained from CGH arrays

Sfpi1/PU.1 R235	Amino acid change	No. of samples (%)	Chr 2 del
CGC>TGC	Arg→Cys	40 (32)	Del 36, retained 2, unknown 2
CGC>CAC	Arg→His	29 (24)	Del 26, retained 2, unknown 1
CGC>AGC	Arg→Ser	11 (9)	Del 10, unknown 1
CGC>CTC	Arg→Leu	3 (2)	Del 3, retained 0
CTGCGC>CTATGC	Leu, Arg→Leu, Cys	1 (1)	Unknown 1
None (CGC)	None	39 (32)	Del 19, retained 18, unknown 2
Flt3 Exon 14	Insertion	No. of Samples (%)	
Insertions	DFYVDFKDY[a] HFYVDFRDYEY[a] VKMLKE[b] FYVDFRDY NFRDYEYDLKW	5 (4)	Retained 5
No insertion	–	119 (96)	Del 95, retained 17, unknown 7
Kras G12	Amino acid change	No. of samples (%)	
GGT>GAT	Gly>Asp	2 (2)	Deletion 2
GGT>CGT	Gly>Arg	1 (1)	Retained 1
None (GGT)	None	120 (97)	Del 93, retained 20, unknown 7

[a]Previously published in Finnon et al. (17).
[b]Previously published in Finnon et al. (17) and only Flt3-ITD information included. Percentages for Flt3-ITD are calculated from 124 mice.

by leucocytosis, splenomegaly and increased leukaemic blasts in the peripheral blood and bone marrow (28). A novel amino acid change of Gly→Arg was also found in one mouse. Similarly, in humans a G12D mutation has been the most commonly reported (23,25), with a G12R mutation being less frequently mutated (24). To the best of our knowledge, this is the first time a *Kras* G12R mutation, previously reported in human AML (29), has been reported in the mouse. Other common human AML mutations were not identified here. As the CBA mouse is an inbred strain it is not probably to represent the full variability of human AML development. However, only hotspots of mutations and frame shifts were studied and so the genes could still be altered by other mutations or epigenetic mechanisms so far unidentified.

Pyrosequencing analysis allowed accurate quantification of *Sfpi1* mutation levels in the three *Kras* G12 mutated AML cases. An *Sfpi1* R235 mutation occurred in 70% of the sample in both case 1 and case 2 suggesting that it is the first driver mutation whereas the *Kras* mutations occurred at a lower frequency of 46% in case 1 and 30% in case 2, occurring later in the clonal expansion stage. For case 3 the *Kras* G12R mutation is detected in 39% of the sample but no *Sfpi1* mutation, which suggests that there may be another mechanism driving AML development.

Significant reduction of *Sfpi1* expression evident in wild-type *Sfpi1* R235 AML

Previous work has shown that reduced expression of *Sfpi1* in haematopoietic stem cells and progenitors down to 20% of wild-type levels will result in the development of AML within 3–8 months (30). The transcriptional analysis of rAML samples presented in this study showed a significant reduction of *Sfpi1* expression in the absence of a R235 mutation. Both high and low levels of *PU.1* expression have also been detected in human AML patient samples (31). Will et al. identified common differentially expressed genes in a mouse model of AML and human AML patients with low levels of *PU.1* (31). A significant down-regulation of *Sfpi1* has also been reported by Salemi et al. in *FLT3-ITD* cases in human AML samples (32). In our *Flt3*-ITD samples, however this was not seen as two cases had a low expression of *Sfpi1* whereas two cases had a high expression of *Sfpi1* in comparison with control levels. This difference in transcriptional expression may be due to the CBA/H and F1 CBA/H × C57BL/Lia strain differences between samples, however more samples would be needed to confirm this. Repression of *Sfpi1* expression could therefore be the driver of AML development in cases without a R235 mutation. We next investigated which epigenetic mechanisms could be responsible for this repression of *Sfpi1*.

Identification of microRNA upregulated in *Sfpi1* R235 mutated AML

We identified two new miRNA, using the nCounter system and validated by QPCR. Both *miR-582-5p* and *miR-1983* were significantly up-regulated in *Sfpi1* R235 mutated AML samples in comparison with wild-type *Sfpi1* R235 samples, suggesting that the role of these microRNA appear to be linked with *Sfpi1* AML pathway.

The increase in *miR-1983* may be due to hypokalaemia, which is frequently seen in AML cases and can result in a decrease in the hormone alderstone, a regulator of miR-1983 (33). Both up and down-regulation of *miR-582-5p* has been reported in several cancers, including acute lymphoblastic leukaemia (ALL) studies (34–36). *miR-582-3p* inhibits negative regulators of the Wnt/β-catenin signalling pathway such as *AXIN2*, *DKK* and *SFRP1* (37) and so the high expression of *miR-582-5p* in samples with an *Sfpi1* R235 mutation indicate that the Wnt pathway is possibly activated in these samples. For AML development, the expression of *miR-582-3p* and *miR-582-5p* in human lung cancer samples with an activated Wnt/β-catenin signalling pathway

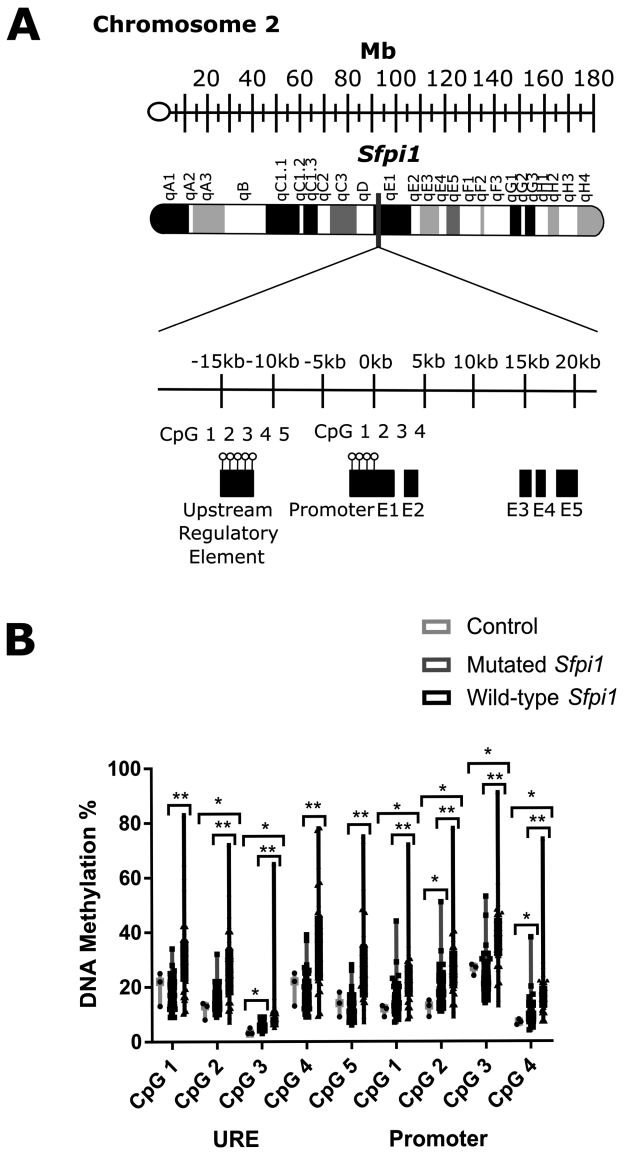

Figure 4. Genomic location of methylated CpG sites in *Sfpi1* in the mouse. (**A**) *Sfpi1* is located on chromosome 2 (2qE1). The gene *Sfpi1* consists of five exons (E1–E5) and two upstream regions which control its expression, an upstream regulatory element which is located 14 kb upstream of the transcription start site and a promoter region. Five CpG sites were analysed in the upstream regulatory element whereas four CpG sites were analysed in the promoter. (**B**) DNA methylation was measured in 3 CBA bone marrow control samples, 69 samples mutated in codon R235 and 35 wild-type codon R235 samples by pyrosequencing at 5 CpG sites in the upstream regulatory element and 4 CpG sites in the promoter region. Significance was calculated by performing a Mann–Whitney test on gene expression data and indicated with an asterisk (* $P \leq 0.05$, ** $P \leq 0.001$).

(38) is of particular interest as activation of the Wnt/β-catenin signalling pathway is essential in the development of leukaemic cells (39,40).

miRNA analysis of *miR-155* was also analysed as it has been previously reported to target *Sfpi1* mRNA for downregulation (41). It has previously been suggested to have an oncogenic role being upregulated in B-cell lymphoma (42), Hodgkin lymphoma (43), AML with *FLT3*-ITD mutations (44) with sustained expression of *miR-155* in mice HSCs producing a myeloproliferative disorder (45) but more recently, evidence of an anti-leukaemic role has been also identified by induction of apoptosis and differentiation (46). Despite our efforts, we were unable to confirm an increased expression of *miR-155* in samples with an *Flt3*-ITD in comparison with other rAML samples as reported in Salemi et al. (32). An up-regulation in *miR-155* expression, although not significant, was seen in wild-type *Sfpi1* R235 samples. As a negative regulator of *Sfpi1* expression, this microRNA may have a role in the down regulation of *Sfpi1* expression, however, it does not appear to be the main cause in rAML cases.

DNA methylation levels are higher at CpGs upstream of *Sfpi1* in wild-type R235 cases

To assess if other epigenetic modifications were responsible for the overall lower expression of wild-type *Sfpi1* R235 samples, site specific DNA methylation analysis was also performed for *Sfpi1*. Expression of *Sfpi1* is maintained by a promoter and by a highly conserved URE, a kb-14 site in mice (18) corresponding to a kb-17 site in humans (47). The URE is necessary for expression of *Sfpi1* as knock out of this region results in the reduction of *Sfpi1* expression to 20% of its wild-type level with the development of AML (30). Previous epigenetic analyses revealed that the promoter and −17 kb URE of *PU.1* is highly methylated in human classical Hodgkin lymphoma cells (48), human myeloma cells (47) and murine erythroleukaemia cells (49,50). Here, DNA methylation analysis of the four CpG sites in the promoter region and five CpGs in the URE demonstrated an up-regulation in all CpG sites for AML cases in comparison with controls, whereas all sites had a significant up-regulation in DNA methylation in wild-type *Sfpi1* R235 samples in comparison with mutated samples. In case 3, the methylation level was very high at all CpG sites, reaching 91% hence suggesting that the high level of DNA methylation, could repress transcriptional expression and may represent the main first event of leukaemogenesis in the absence of an *Sfpi1* mutation. Although not a dominant pathway in murine AML, repression of *Sfpi1* appears to be an alternative pathway disrupting myeloid development and may also be a driver of AML development in human cases. Further analysis of *Sfpi1* transcriptional and methylation levels in larger AML patient cohorts, particularly rAML if possible, will be necessary to confirm this.

Although a rare event, the development of AML in case 3 clearly seems to involve *Sfpi1* disruption through promoter DNA methylation and transcriptional repression followed by a *Kras* G12R mutation, reported for the first time in the CBA mouse (Supplementary Figure S2 is available at *Carcinogenesis* Online). To summarize, we identified new pathways of radiation leukaemogenesis (Figure 5). The major pathway consists of a described previously chromosome 2 deletion with an *Sfpi1* R235 mutation, which occurs predominantly in male mice. A sub-pathway reveals that AML can develop where there is a chromosome 2 deletion and significant increase in *Sfpi1* DNA methylation with reduction of *Sfpi1* transcriptional expression in the absence of a R235 mutation. A newly identified minor pathway neither requires chromosome 2 deletion nor *Sfpi1* R235 mutation, but rather a significant increase in *Sfpi1* DNA methylation with reduction of *Sfpi1* transcriptional expression and this occurs predominantly in female cases. Minor pathways include *Flt3*-ITD, *Sfpi1* R235 or *Kras* G12 mutations. The cases of *Flt3*-ITD clearly appear to have a gender bias with all cases so far, 4 seen here a fifth case reported in Finnon et al. but not analysed here, presenting in females. The minor pathway presenting in case 3 represents a novel pathway consisting of site specific DNA methylation associated with reduced *Sfpi1* transcription and a *Kras* G12 mutation.

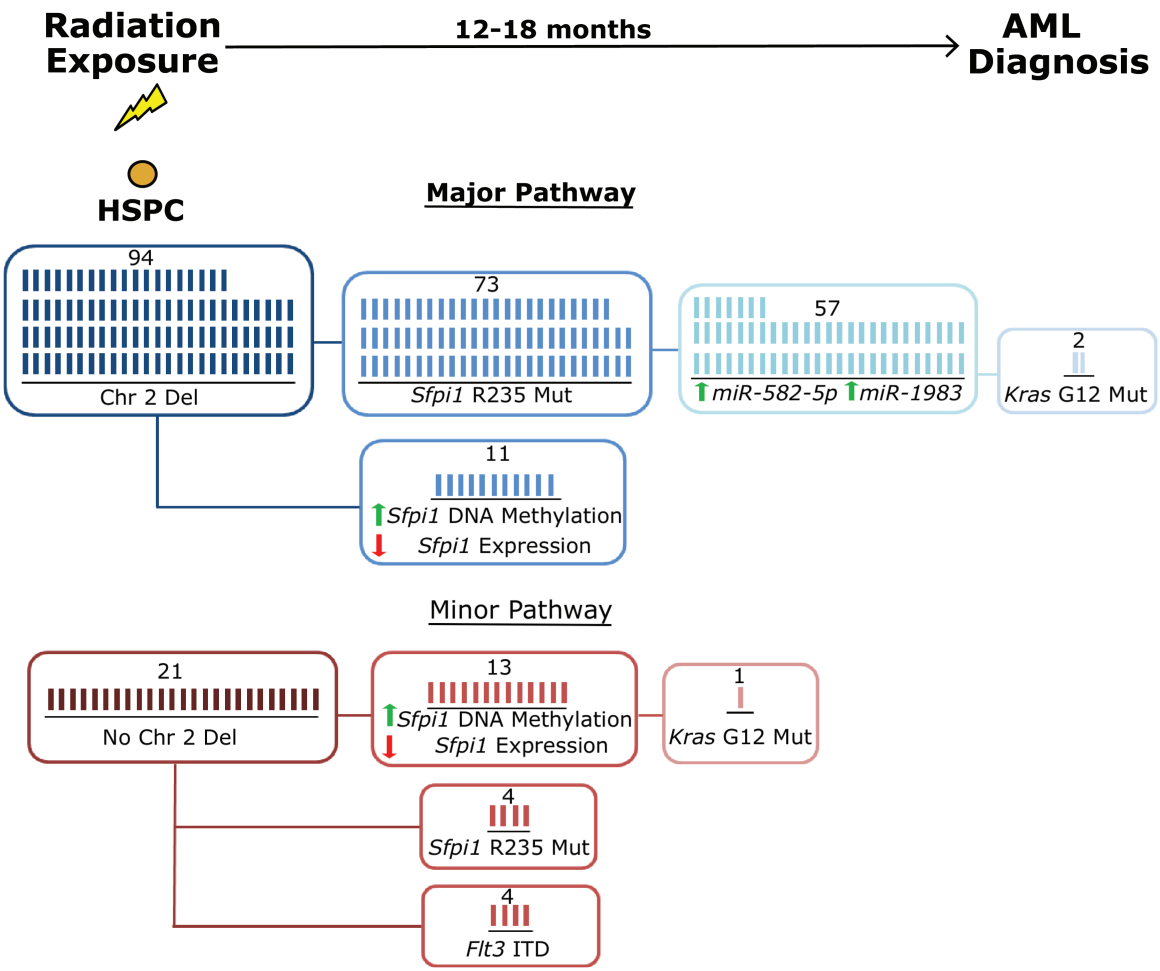

Figure 5. Genetic and epigenetic pathway analysis of rAML. After irradiation exposure, there appears to be at least two pathways of rAML development. The major pathway consists of a chromosome 2 deletion with an *Sfpi1* R235 mutation whereas the minor pathway consists of no chromosome 2 deletion and no *Sfpi1* R235 mutation but instead a significant increase in *Sfpi1* DNA methylation and reduction of *Sfpi1* transcriptional expression.

Overall this work provides new insight into the pathways leading to rAML development, involving genetic mutations as well as epigenetic changes and, for the first time, specific gene DNA methylation.

Supplementary material

Supplementary data are available at *Carcinogenesis* online.

Authors contribution

JZ and JP designed the algorithms and performed numerical and bioinformatical analyses required within the study.

Acknowledgements

This work was funded by Public Health England and was supported by the European Union FP7 EURATOM DoReMi network of excellence [Grant agreement 249689]; RISK-IR (Risk, Stem Cells and Tissue Kinetics—Ionising Radiation) [Grant agreement 323267]; National Science Centre, Poland, grant BITIMS [Grant agreement 2015/19/B/ST6/01736 to JP]; National Science Centre, Poland, grant SUT BKM [Grant agreement 02/010/BKM18/0136 to JZ]. Neutron irradiations and AML sample collection carried out by M. Sutmuller, E. Meijne and R. Huiskamp at NRG, Petten, The Netherlands.

Conflict of Interest Statement: The authors declare no competing financial interests.

References

1. Hsu, W.L. *et al.* (2013) The incidence of leukemia, lymphoma and multiple myeloma among atomic bomb survivors: 1950–2001. *Radiat. Res.*, 179, 361–382.
2. Schoch, C. *et al.* (2004) Karyotype is an independent prognostic parameter in therapy-related acute myeloid leukemia (t-AML): an analysis of 93 patients with t-AML in comparison to 1091 patients with *de novo* AML. *Leukemia*, 18, 120–125.
3. Rithidech, K. *et al.* (1995) Hypermutability of mouse chromosome 2 during the development of X-ray-induced murine myeloid leukemia. *Proc. Natl. Acad. Sci. U. S. A.*, 92, 1152–1156.
4. Major, I.R. *et al.* (1978) Myeloid leukaemia in X-ray irradiated CBA mice. *Nature*, 272, 455–456.
5. Verbiest, T. *et al.* (2015) *PU.1* downregulation in murine radiation-induced acute myeloid leukaemia (AML): from molecular mechanism to human AML. *Carcinogenesis*, 36, 413–419.
6. Silver, A. *et al.* (1999) Molecular mapping of chromosome 2 deletions in murine radiation-induced AML localizes a putative tumor suppressor gene to a 1.0 cM region homologous to human chromosome segment 11p11-12. *Genes Chromosomes Cancer*, 24, 95–104.
7. Cook, W.D. *et al.* (2004) *PU.1* is a suppressor of myeloid leukemia, inactivated in mice by gene deletion and mutation of its DNA binding domain. *Blood*, 104, 3437–3444.

8. Suraweera, N. *et al.* (2005) Mutations of the *PU.1* Ets domain are specifically associated with murine radiation-induced, but not human therapy-related, acute myeloid leukaemia. *Oncogene*, 24, 3678–3683.
9. Basova, P. *et al.* (2014) Aggressive acute myeloid leukemia in *PU.1*/p53 double-mutant mice. *Oncogene*, 33, 4735–4745.
10. Steidl, U. *et al.* (2006) Essential role of Jun family transcription factors in *PU.1* knockdown-induced leukemic stem cells. *Nat. Genet.*, 38, 1269–1277.
11. Ley, T.J. *et al.*; Cancer Genome Atlas Research Network. (2013) Genomic and epigenomic landscapes of adult *de novo* acute myeloid leukemia. *N. Engl. J. Med.*, 368, 2059–2074.
12. Olme, C.H. *et al.* (2013) Live cell detection of chromosome 2 deletion and Sfpi1/PU1 loss in radiation-induced mouse acute myeloid leukaemia. *Leuk. Res.*, 37, 1374–1382.
13. Brown, N. *et al.* (2015) Influence of radiation quality on mouse chromosome 2 deletions in radiation-induced acute myeloid leukaemia. *Mutat. Res. Genet. Toxicol. Environ. Mutagen.*, 793, 48–54.
14. Kogan, S.C. *et al.* (2002) Bethesda proposals for classification of nonlymphoid hematopoietic neoplasms in mice. *Blood*, 100, 238–245.
15. Bendl, J. *et al.* (2014) PredictSNP: robust and accurate consensus classifier for prediction of disease-related mutations. *PLoS Comput. Biol.*, 10, e1003440.
16. Adzhubei, I.A. *et al.* (2010) A method and server for predicting damaging missense mutations. *Nat. Methods*, 7, 248–249.
17. Finnon, R. *et al.* (2012) Flt3-ITD mutations in a mouse model of radiation-induced acute myeloid leukaemia. *Leukemia*, 26, 1445–1446.
18. Li, Y. *et al.* (2001) Regulation of the *PU.1* gene by distal elements. *Blood*, 98, 2958–2965.
19. Okuno, Y. *et al.* (2005) Potential autoregulation of transcription factor *PU.1* by an upstream regulatory element. *Mol. Cell. Biol.*, 25, 2832–2845.
20. Chen, H. *et al.* (1995) *PU.1* (Spi-1) autoregulates its expression in myeloid cells. *Oncogene*, 11, 1549–1560.
21. Fröhling, S. *et al.* (2002) Prognostic significance of activating FLT3 mutations in younger adults (16 to 60 years) with acute myeloid leukemia and normal cytogenetics: a study of the AML Study Group Ulm. *Blood*, 100, 4372–4380.
22. Yamamoto, Y. *et al.* (2001) Activating mutation of D835 within the activation loop of FLT3 in human hematologic malignancies. *Blood*, 97, 2434–2439.
23. Tyner, J.W. *et al.* (2009) High-throughput mutational screen of the tyrosine kinome in chronic myelomonocytic leukemia. *Leukemia*, 23, 406–409.
24. Stirewalt, D.L. *et al.* (2001) FLT3, RAS, and TP53 mutations in elderly patients with acute myeloid leukemia. *Blood*, 97, 3589–3595.
25. Neubauer, A. *et al.* (1994) Prognostic importance of mutations in the ras proto-oncogenes in *de novo* acute myeloid leukemia. *Blood*, 83, 1603–1611.
26. Illmer, T. *et al.* (2005) Activation of the RAS pathway is predictive for a chemosensitive phenotype of acute myelogenous leukemia blasts. *Clin. Cancer Res.*, 11, 3217–3224.
27. Guerrero, I. *et al.* (1984) Activation of a c-K-ras oncogene by somatic mutation in mouse lymphomas induced by gamma radiation. *Science*, 225, 1159–1162.
28. Kelly, M.J. *et al.* (2019) Bcor loss perturbs myeloid differentiation and promotes leukaemogenesis. *Nat. Commun.*, 10, 1347.
29. Bolouri, H. *et al.* (2018) The molecular landscape of pediatric acute myeloid leukemia reveals recurrent structural alterations and age-specific mutational interactions. *Nat. Med.*, 24, 103–112.
30. Rosenbauer, F. *et al.* (2004) Acute myeloid leukemia induced by graded reduction of a lineage-specific transcription factor, *PU.1*. *Nat. Genet.*, 36, 624–630.
31. Will, B. *et al.* (2015) Minimal *PU.1* reduction induces a preleukemic state and promotes development of acute myeloid leukemia. *Nat. Med.*, 21, 1172–1181.
32. Salemi, D. *et al.* (2015) miR-155 regulative network in FLT3 mutated acute myeloid leukemia. *Leuk. Res.*, 39, 883–896.
33. Edinger, R.S. *et al.* (2014) Aldosterone regulates microRNAs in the cortical collecting duct to alter sodium transport. *J. Am. Soc. Nephrol.*, 25, 2445–2457.
34. Zhang, H. *et al.* (2009) MicroRNA patterns associated with clinical prognostic parameters and CNS relapse prediction in pediatric acute leukemia. *PLoS One*, 4, e7826.
35. Schotte, D. *et al.* (2009) Identification of new microRNA genes and aberrant microRNA profiles in childhood acute lymphoblastic leukemia. *Leukemia*, 23, 313–322.
36. de Oliveira, J.C. *et al.* (2012) MicroRNA expression and activity in pediatric acute lymphoblastic leukemia (ALL). *Pediatr. Blood Cancer*, 59, 599–604.
37. Fang, L. *et al.* (2015) Aberrantly expressed miR-582-3p maintains lung cancer stem cell-like traits by activating Wnt/β-catenin signalling. *Nat. Commun.*, 6, 8640.
38. Jin, X. *et al.* (2017) Crosstalk in competing endogenous RNA network reveals the complex molecular mechanism underlying lung cancer. *Oncotarget*, 8, 91270–91280.
39. Staal, FJ *et al.* Aberrant Wnt signaling in leukemia. *Cancers (Basel)*. 2016;8.
40. Wang, Y. *et al.* (2010) The Wnt/beta-catenin pathway is required for the development of leukemia stem cells in AML. *Science*, 327, 1650–1653.
41. Gerloff, D. *et al.* (2015) NF-κB/STAT5/miR-155 network targets *PU.1* in FLT3-ITD-driven acute myeloid leukemia. *Leukemia*, 29, 535–547.
42. Eis, P.S. *et al.* (2005) Accumulation of miR-155 and BIC RNA in human B cell lymphomas. *Proc. Natl. Acad. Sci. U. S. A.*, 102, 3627–3632.
43. Kluiver, J. *et al.* (2005) BIC and miR-155 are highly expressed in Hodgkin, primary mediastinal and diffuse large B cell lymphomas. *J. Pathol.*, 207, 243–249.
44. Faraoni, I. *et al.* (2012) MiR-424 and miR-155 deregulated expression in cytogenetically normal acute myeloid leukaemia: correlation with NPM1 and FLT3 mutation status. *J. Hematol. Oncol.*, 5, 26.
45. O'Connell, R.M. *et al.* (2008) Sustained expression of microRNA-155 in hematopoietic stem cells causes a myeloproliferative disorder. *J. Exp. Med.*, 205, 585–594.
46. Palma, C.A. *et al.* (2014) MicroRNA-155 as an inducer of apoptosis and cell differentiation in acute myeloid leukaemia. *Mol. Cancer*, 13, 79.
47. Tatetsu, H. *et al.* (2007) Down-regulation of *PU.1* by methylation of distal regulatory elements and the promoter is required for myeloma cell growth. *Cancer Res.*, 67, 5328–5336.
48. Yuki, H. *et al.* (2013) *PU.1* is a potent tumor suppressor in classical Hodgkin lymphoma cells. *Blood*, 121, 962–970.
49. Shearstone, J.R. *et al.* (2011) Global DNA demethylation during mouse erythropoiesis in vivo. *Science*, 334, 799–802.
50. Fernández-Nestosa, M.J. *et al.* (2013) DNA methylation-mediated silencing of *PU.1* in leukemia cells resistant to cell differentiation. *Springerplus*, 2, 392.